
Immersed borders approach for fluid-structure interaction

Chaib Kkaled¹, Sahli Ahmed^{2,*}, Sara Sahli³

1. *Laboratoire de recherche des technologies industrielles, Université Ibn Khaldoun de Tiaret, Département de Génie Mécanique, BP 78, Route de Zaroura, Tiaret 14000, Algérie*
2. *Laboratoire de Mécanique Appliquée, Université des Sciences et de la Technologie d'Oran (USTO MB), Oran, Algeria*
3. *Université d'Oran 2 Mohamed Ben Ahmed, Oran, Algeria*

mechanics184@yahoo.com

ABSTRACT. *In this paper, a formulation using the Generalized Finite Element Method (GFEM) in conjunction with Lagrange Multipliers is proposed to impose the boundary condition on the interface of the Fluid-Structure Interaction (FSI) problem. The objective of this work is the development of an efficient and robust computational code for solving problems of Fluid Mechanics and FSI. We chose a formulation of Immersed Borders to allow simulations of problems involving complex movements and transformations of the structure. In problems with these characteristics, classical ALE approaches tend to lose robustness because of the need for fluid mesh reconstruction to avoid excessive distortion of the elements. Examples of future applications are biomechanics, aeroelasticity of civil works and aerospace and multiphysical structures. The numerical examples solved proved that the formulation and implementation in finite elements developed in this work are capable to solve problems of 2D flow of fluids described by the Navier-Stokes equation for incompressible flows, even in regimes with dominant convection; and, to simulate the fluid problems with mobile interfaces using the concept of boundaries immersed in two dimensions.*

RÉSUMÉ. *Dans cet article, une formulation utilisant la méthode généralisée des éléments finis (GFEM) en conjonction avec les multiplicateurs de Lagrange est proposée pour imposer la condition de limite à l'interface du problème d'interaction fluide-structure (FSI). L'objectif de ce travail est de développer un code informatique efficace et robuste pour résoudre les problèmes de mécanique des fluides et de FSI. Nous avons choisi une formulation de Immersed Borders pour permettre la simulation de problèmes impliquant des mouvements complexes et des transformations de la structure. En cas de problèmes avec ces caractéristiques, les approches classiques ALE ont tendance à perdre de la robustesse en raison de la nécessité de reconstruire un maillage fluide pour éviter une distorsion excessive des éléments. Des exemples d'applications futures sont la biomécanique, l'aéroélasticité des travaux de génie civil et les structures aérospatiales et multiphysiques. Les exemples numériques résolus ont prouvé que la formulation et la mise en œuvre d'éléments finis développées dans ce travail sont capables de résoudre les problèmes d'écoulement 2D de*

fluides décrits par l'équation de Navier-Stokes pour les écoulements incompressibles, même dans des régimes à convection dominante; et, pour simuler les problèmes fluides avec les interfaces mobiles en utilisant le concept de frontières immergées dans deux dimensions.

KEYWORDS: generalized finite element method, mobile interfaces, incompressible flows

MOTS-CLÉS: methode generalisee des elements finis, interfaces mobiles, ecoulements incompressibles

DOI:10.3166/ACSM.41.109-126 © 2017 Lavoisier

1. Introduction

Fluid-Structure Interaction Problems (FSI) is of great importance for engineering and is present both in nature and in works and machines built by man. This is a problem involving Fluid Mechanics and Structures and in which the solution of one domain depends on the solution of the other, thus characterizing a coupled system. If solving a fluid mechanics problem with diverse boundary conditions is already a difficult task, an FSI problem adds as a challenge the simultaneous solution of the coupled system in which the boundary conditions at the interface between the fluid and the structure are unknown a priori, because they depend on the solution of the problem. In addition, because most engineering concerns involve large displacements of fluid structure and convection, FSI is by nature a strongly non-linear problem.

The nature of FSI problems can be very varied. Offshore structures such as oil exploration platforms of interest to Civil Engineering and Petroleum are typical examples involving FSI. In these cases, a problem formulation capable of representing the free surface of the fluid is required, and in some situations it is also interesting to be able to simulate the contact between the floating structures. This line of study today attracts several research groups in the world (Akkerman *et al.*, 2012; Buscaglia and Ausas, 2011; Marrone *et al.*, 2011; Lins *et al.*, 2010; Elias *et al.*, 2009; Takizawa *et al.*, 2007; Dettmer and Peric 2006; Löhner *et al.*, 2006; Kulasegaram *et al.*, 2004; Braess and Wriggers, 2000; Feng and Peric, 2000) due to the opportunity of oil exploration in deep waters.

From a numerical point of view, when there is fluid and structure with similar densities, as is the case with blood and arteries of the human body, the FSI problem requires special care to control possible instabilities in the resolution of the coupled system (Küttler and Wall 2008; Förster *et al.*, 2007). Other difficulties inherent to this type of simulation are the acquisition of images of the patient to generate the geometric model, to establish the initial condition of the FSI problem, to define the profile of velocities at the border of entry of the flow, among others. For further references of biomechanical works, the reader will find in (Tezduyar *et al.*, 2011; Torii *et al.*, 2011; Torii *et al.*, 2009; Torii *et al.*, 2007; Maier *et al.*, 2010; Takizawa *et al.*, 2010; Bazilevs *et al.*, 2009; Bazilevs *et al.*, 2008) works also on cerebral aneurysm, influence of blood pressure and aneurysm geometry on the risk of rupture of the simulation of cardiac valves and artificial blood pumping in patients with heart failure.

Because of the varied nature of FSI problems, it is difficult to imagine that a particular approach or method is superior in all classes of problems. In fact, many computational programs, commercial or academic, lose robustness in certain problems that involve complex transformations of the structure, with large displacements or rotations, or problems whose interface between the fluid and the structure is complicated, just to mention a few examples.

In general, the numerical methods currently available for solving FSI problems can be classified into two large groups depending on the way they treat the interface between the fluid and the structure: coincident boundary methods and immersed boundary methods.

The coincident boundary methods use in their formulation the approach ALE (Arbitrary Lagrangian Eulerian), in which the fluid problem is formulated and solved from a mesh that deforms to follow the movement of the structure. This is due to the fact that the fluid network is constructed by limiting itself to the physical domain of the fluid. In this way, the mesh of the fluid deforms following the deformation of the structure at the interface and this deformation propagates in a predefined region of the fluid. Since the mesh of the fluid is connected to the wet surface of the structure, it cannot be preserved when the structure undergoes complex transformations and therefore the generation of a new mesh is unavoidable. Alternatively, methods that rely on the concept of immersed boundaries treat the fluid and structure from two superimposed domains. The meshes are independently constructed and therefore the fluid can conveniently be solved using a fixed and undeformable mesh in a classical Eulerian approach. The structure, in turn, is solved Lagrangian as usual. As the fluid and structure meshes are independently constructed, some special technique is required to impose the effect of the movement of the wetted surface of the structure on the fluid, since the movement of this interface acts as an essential contour condition to the fluid. However, in general, there are no knots of the fluid mesh along the interface for this boundary condition to be imposed directly, usual practice of the finite element method.

It is also possible to think of a method that treats the fluid and the structure from a unified Lagrangian approach. This method, developed by Oñate and Idelson (Oñate *et al.*, 2008; Idelson *et al.*, 2001; Idelson *et al.*, 2008; Idelson *et al.*, 2006; Oñate and García, 2001) and called the particle method, is very interesting in applications involving fluid flow with free surface and detachment of part of the fluid domain in sub domains, a common phenomenon in waves impact situations in offshore structures or sea breaking. The great advantage of this approach lies in the elimination of the convective term of the equation that describes the movement of the fluid, but the price of generating a new mesh for each increment of time of the simulation is paid.

Several other techniques have been researched with the same objective of imposing Dirichlet boundary conditions along with immersed boundary methods. We highlight the Distributed Lagrange Multipliers method (Zilian and Legay, 2008; Zhaosheng, 2005), in which the Lagrange Multipliers are defined at the nodes of the fluid elements cut by the interface, variations of the Nitsche method (Rüberg and

Cirak, 2012; Sanders *et al.*, 2012), mixed hybrid methods in the which fluid elements intersected by the interface are enriched with an additional tensile field to ensure the imposition of the Dirichlet condition on the interface (Baiges *et al.*, 2012; Gerstenberger and Wall, 2010; Zilian and Fries, 2009) and discontinuous Galerkin methods (Lew and Buscaglia, 2008).

In this work, it is proposed a Fluid-Structure Interaction method based on an immersed interface approach in opposition to classical ALE (*Arbitrary Lagrangian Eulerian*) approaches. Generalized Finite Elements, together with Lagrange Multipliers, are used to provide velocity and pressure discontinuities on the fluid domain across the immersed interface. To couple both fluid and structural problems, an implicit staggered scheme is adopted, which allows the easy implementation of already developed black box computer codes.

2. Problem of fluid-structure interaction

In this section, the formulation used to solve the coupled fluid-structure interaction (FSI) problem will be described. This formulation uses the concept of immersed boundaries as an alternative to classical ALE formulations.

2.1. Introduction

The basic idea is to use GFEM in conjunction with Lagrange multipliers to impose the boundary conditions at the interface between the fluid and the structure and was originally proposed in (Gerstenberger and Wall, 2008; Legay *et al.*, 2006). This technique solves the problem of fluids from a fixed Eulerian mesh in which elements interrupted by the boundary of the structure are enriched to provide the necessary discontinuities in speed and pressure. In addition, in general, the boundary of the frame does not coincide with the nodes of the mesh of the fluid and therefore the speed of the fluid in this interface must be imposed on the weak form of the problem. In order to formulate the coupled FSI problem, some definitions become necessary. Let Ω be the domain of computation containing the structural domain Ω^s and the fluid domain Ω^f , which extends partially or totally on the domain Ω^s so that $\Omega^f \cap \Omega^s \neq \emptyset$.

The indices 's' and 'f' will be used to distinguish between the magnitudes of the structure and the fluid respectively, and will be omitted when there is no need.

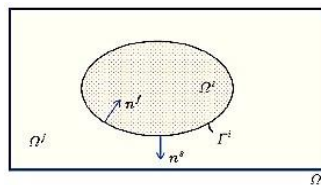


Figure 1. Definition of domains in the coupled problem

Figure 1 shows the domains of the fluid and structure just defined as well as their respective unit normal vectors n^f and n^s at the interface Γ^i .

The interface Γ^i , also referred to as the "wet surface", in turn, divides the fluid domain into two new subsets that will be called Ω^+ and Ω^- , the second without any physical meaning and called a fictitious domain. The decomposition of Ω^f into Ω^+ and Ω^- occurs through a disjunction bipartition, that is, $\Omega^f = \Omega^+ \cup \Omega^-$ and $\Omega^+ \cap \Omega^- = \emptyset$.

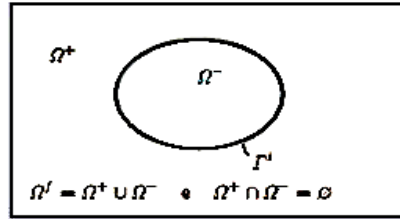


Figure 2. Decomposition of the fluid domain in Ω^+ and Ω^-

Figure 2 illustrates these new domains. It is worth remembering that during numerical computation of the problem, the finite elements of fluid belonging to Ω^- will be deactivated, thus avoiding an unnecessary increase in computational cost of processing and memory required to solve the problem.

2.2. Imposition of interface conditions

The conditions that need to be satisfied in the interface can be written as

$$u^f = u^s \quad \forall x \in \Gamma^i \quad (1)$$

$$T^f n^f = -T^s n^s \quad \forall x \in \Gamma^i \quad (2)$$

Eq. (1) establishes a kinematic adhesion condition consisting of equal fluid and structure velocities along the interface while eq. (2) is a dynamic condition, which imposes the balance of forces on Γ^i . This balance of forces comes down to equal stress since the surface area on which these forces act is the same. The opposite sign is due to the inverted orientation of the normal vectors according to Figure 1.

2.3. The fluid problem with mobile interfaces

If we assume that the transformation, or movement, of the structure is known priori, the coupled IFE problem is reduced to a fluid problem with mobile interfaces. In this way, we can rewrite conditions (1) and (2) as

$$u^f = \bar{u}^{-i} \quad \forall x \in \Gamma^+ \tag{3}$$

$$t^f = 0 \quad \forall x \in \Gamma^- \tag{4}$$

Where the positive or negative sign of Γ refers to where we approach the interface, if by Ω^+ or Ω^- , respectively. \bar{u}^{-i} is the speed of the mobile interface. Note that with these definitions, we have Dirichlet boundary conditions at the interface of Ω^+ and boundary conditions of the Neumann type in the contour of the dummy domain Ω^- . Imposing still the following initial conditions to the fictitious domain of the fluid

$$\begin{aligned} u(x, t = 0) &= 0 \quad \forall x \in \Omega^- \\ p(x, t = 0) &= 0 \quad \forall x \in \Omega^- \end{aligned} \tag{5}$$

and assuming that there are no volume forces in this domain, it is guaranteed that there will be no flow in Ω^- throughout the simulation of the problem. Satisfying the conditions of (3) to (5), however, requires discontinuous velocity and pressure fields. This discontinuous field will be provided during the discretization of the problem in space. The imposition of the condition (3) is done via Lagrange Multipliers see (Sawada and Tezuka, 2010; Turek *et al.*, 2010; Gerstenberger and Wall, 2008; Legay *et al.*, 2006; Moës *et al.*, 2006). You can then define a function given by

$$\pi = \int_{\Gamma^+} \lambda \cdot (u - \bar{u}^{-i}) d\Gamma^+ \tag{6}$$

where λ , represents the Lagrange Multipliers of the condition (3) and, therefore, constitutes an additional unknown to the problem. By a dimensional analysis, we conclude that λ is a stress applied along Γ^+ , in turn enabling a physical interpretation of a voltage exerted by the immersed interface so that the fluid flow satisfies (3). The variation of (6) provides

$$\delta\pi = \int_{\Gamma^+} \delta\lambda \cdot (u - \bar{u}^{-i}) d\Gamma^+ + \int_{\Gamma^+} \lambda \cdot \delta u d\Gamma^+ \tag{7}$$

Finally, by introducing the terms obtained in the contour Γ^+ of equation (7) in the weak form of the system of semi-discrete equations of the viscous incompressible flow, we have

$$\begin{aligned} &\left\{ (w, u)_{\Omega^f} + \gamma \Delta t \left[c(u; w, u)_{\Omega^f} + a(w, u)_{\Omega^f} - \right. \right. \\ &\left. \left. (divw, p)_{\Omega^f} + (q, divu)_{\Omega^f} - (w, b)_{\Omega^f} - (w, \bar{t})_{\Gamma_i} - (w, \lambda)_{\Gamma^+} - (\delta\lambda, u - \bar{u}^{-i})_{\Gamma^+} \right] \right\}^{n+1} \\ &= (w, u^n)_{\Omega^f} + (1 + \gamma) \Delta t (w, \dot{u}^n)_{\Omega^f} \end{aligned} \tag{8}$$

where the variation of the velocities, δu , was replaced by the weight function w only for the purpose of uniformity of the notation.

2.4. Discretization of the interface

The Lagrange Multipliers λ and its test function $\delta\lambda$ need to be discretized along the interface Γ . An intuitive way to do this is to define nodes at the intersections between the interface and the sides of the fluid mesh elements, as suggested in (Gerstenberger and Wall 2008). Figure 3 schematically illustrates how the interface is discretized in this approach. Lagrange Multipliers are therefore approximated by shape functions that use the nodes symbolized by triangles in Figure 3 for interpolation. Thus, the Lagrange Multipliers approach and test functions can be defined by

$$\lambda^h = \bigcup_{e=1}^{Nel} N_{\lambda} \lambda_e \quad \delta\lambda^h = \bigcup_{e=1}^{Nel} N_{\lambda} \delta\lambda_e \quad (9)$$

The discretization of the interface shown in Figure 3 has some drawbacks with respect to implementation and numerical instability, especially when finite elements with low order interpolation functions are used in the formulation of the fluid problem. This fact has already been pointed out in (Gerstenberger and Wall, 2008; Moës *et al.*, 2006), since the combination of the λ approach subspace with the velocity and pressure subspaces may be incompatible (LBB) and therefore generate numerical instabilities. The alternative suggested in this work is the construction of an interface mesh independent of the fluid (technique indicated in (Sawada and Tezuka 2010)) in conjunction with discontinuous approximation functions for interpolation of the Lagrange Multipliers in order to make flexible the choice of the subspace dimension approach and facilitate the calculation of the terms to be integrated throughout the interface.

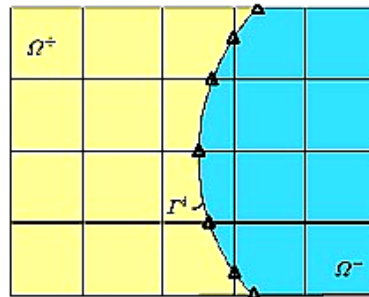


Figure 3. Discretization of the interface defining nodes at the intersection between Γ and fluid elements

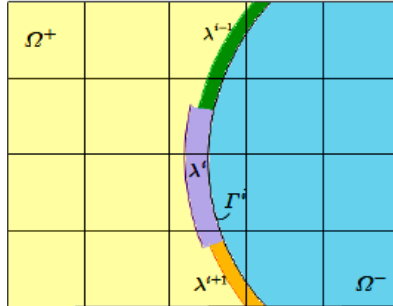


Figure 4. Discretization of the interface using discontinuous and constant functions inside the elements. The interface mesh is constructed independent of the fluid mesh

2.5. The coupled problem

Eliminating the hypothesis of the previous section that the structure transformation is known a priori, some algorithm is necessary in order to solve the coupled problem. We have opted for a staggered scheme that, despite having a generally slower convergence rate when compared to so-called monolithic methods, has its advantage in the possibility of using ready-made computational programs of the structural problem without the necessity of modification.

3. Numerical simulations

In this section, we will present some results of numerical simulations conducted with the objective of verifying the formulations presented.

3.1. Stationary flow around a cylinder ($Re=20$)

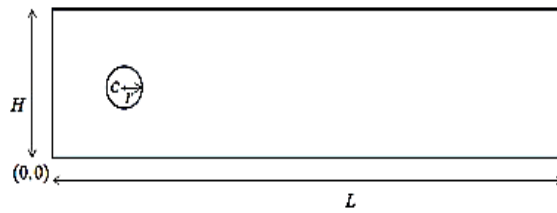


Figure 5. Stationary flow around a cylinder

This is a classic example of literature and can be found in several bibliographical references. See (Tezduyar and Osawa, 2000; Zienkiewicz and Taylor, 2000; Schäfer

and Turek, 1996; Brooks and Hughes, 1982), for example. However, for the purpose of verifying the formulation presented so far, the parameters of reference (Schäfer and Turek, 1996) will be used, since this reference brings together several results of simulations of the problem carried out by several active research groups. The flow is through a narrow channel, see Figure 5, of length $L = 2,2$ m and height $H = 0,41$ m, with origin of the reference system in the lower left corner. Near the entrance of the channel, there is a circular section obstacle with radius $r = 0,05$ m and center positioned in the coordinates $C = (0,20, 0,20)$.

This time, however, the entire domain of the problem has been discretized with finite elements of fluid and therefore the boundary between the fluid and the structure, in the case of the cylinder, is immersed. This fact can be seen in Figure 6 for the Taylor-Hood element Q2Q1 and in Figure 7 for the Taylor-Hood elements P2P1 and P2P1i.

In the case of the Taylor-Hood element Q2Q1, the interface was discretized by creating nodes at the intersections of this with the sides of the fluid elements, as shown in Figure 3 and using linear interpolation functions. The cylinder was considered as a rigid body and therefore did not have to be discretized. The interface, in turn, was internally defined in the computational code due to its geometric simplicity. The velocity and pressure results obtained with the Q2Q1 element can be seen in Figure 8 and Figure 9, respectively.

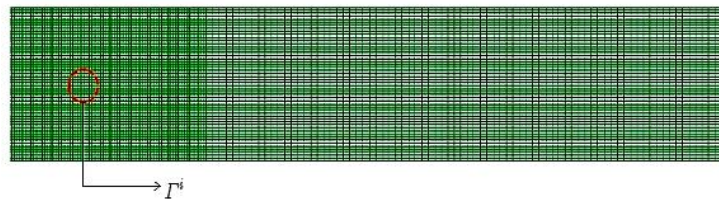


Figure 6. Fluid mesh used in the simulation of Problem 5.1. 23049 Taylor Hood elements Q2Q1 and 92825 nodes

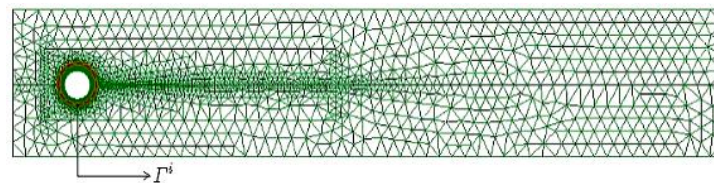


Figure 7. Fluid mesh used in the simulation of Problem 5.1. 7914 elements Taylor Hood P2P1 (or P2P1i) and 16090 nodes

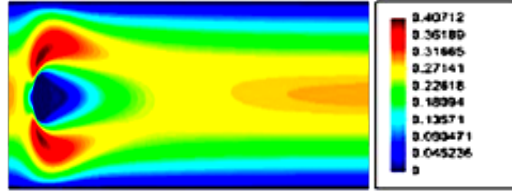


Figure 8. Velocity field obtained with Taylor-Hood finite element Q2Q1

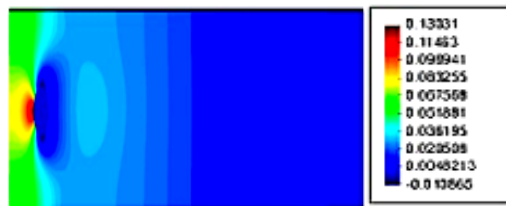


Figure 9. Pressure field obtained with Taylor-Hood finite element Q2Q1

In Figure 10, the pressure distribution around the cylinder is shown in detail. The reader may note that the pressure has not been properly interpolated by the post-processor, causing a false impression that the pressure distribution is not smooth along the cylinder contour. This is due to the fact that the post-processor does not have implemented the enrichment functions.

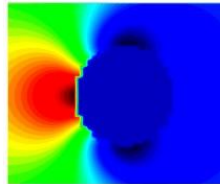


Figure 10. Detail of the pressure distribution along the contour of the cylinder obtained with the finite element Taylor-Hood Q2Q1

However, it is possible to calculate the pressure in the cylinder contour internally in the computational code, using the enriched form functions. This result is shown in Figure 11 along with the Lagrange Multipliers.

It is clearly seen from Figure 11 (a) that the pressure distribution is smooth around the cylinder and is in very good agreement with literature results (see comparison of results below in Table 6. In Figure 11 (b) it is also noticed that there is no evidence of numerical instability due to the incompatibility of the subspaces used in this problem.

In attempting to solve this same problem using other finite elements of fluid with smaller degree interpolation functions, especially the elements P2P1 and P2P1i, phenomena of numerical instability were evidenced. These instabilities, however, were eliminated by discretizing the interface independently of the fluid mesh and having functions in a discontinuous and constant manner within the element, as described in section 2.4 and illustrated in Figure 4. The results obtained for the Lagrange Multipliers are shown in a comparative manner in Figure 12. The drag coefficients c_L and trawl c_D , were also calculated and the results are shown in Table 1.

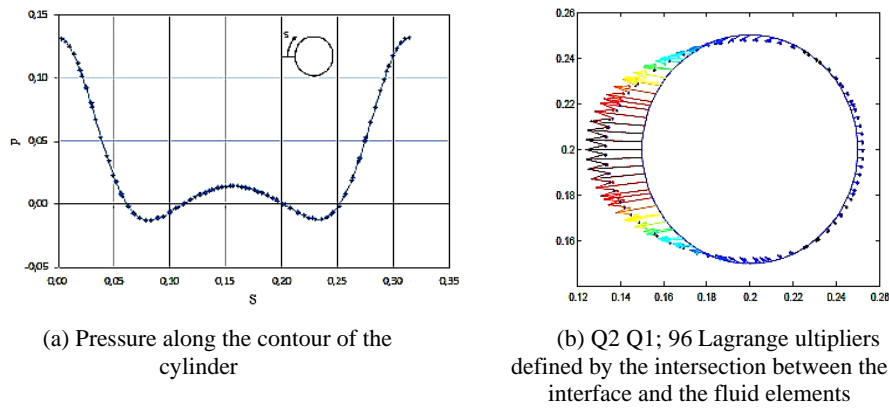


Figure 11. (a) Pressure on the contour of the cylinder and (b) Lagrange multipliers obtained with the Taylor-Hood element Q2Q1

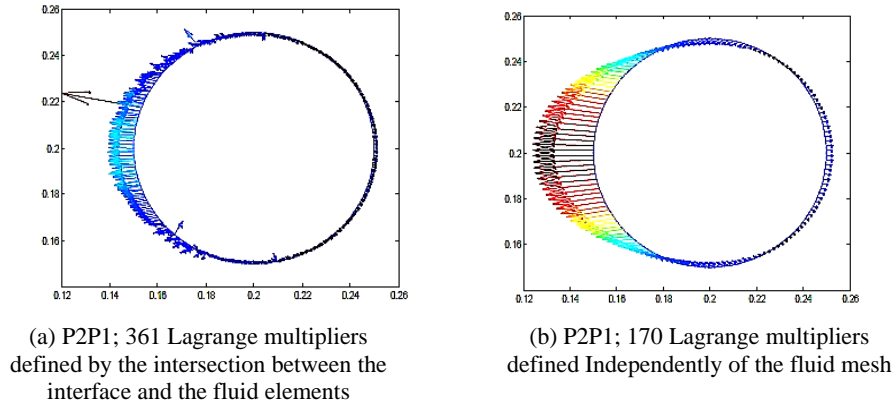


Figure 12. Lagrange multipliers obtained with the elements P2P1 and P2P1i. Comparison between the interface discretization techniques presented in 2.3

Table 1. Comparison of the results obtained with the elements Q2Q1, P2P1 and P2P1i and results of (Schäfer and Turek 1996) for the case of steady flow

	c_L	c_D	ΔP
Q2Q1 with 96 Lagrange Multipliers in the interface	0,0106	5,5759	0,1172
P2P1 with 361 Lagrange multipliers in the interface	0,0096	5,5812	0,1174
P2P1 with 170 Lagrange Multipliers in the interface	0,0107	5,5867	0,1173
P2P1i with 361 Lagrange multipliers in the interface	0,0083	5,5899	0,1185
P2P1i with 150 Lagrange Multipliers in the interface	0,0104	5,5903	0,1174
[R. Rannacher, S. Turek]	0,0106	5,5755	0,1173

3.2. flow around a moving cylinder ($Re=100$)

This example was conducted in two steps. Initially, the cylinder was held fixed until the flow reached periodic regime with alternating vortexing. In the second step, a vertical movement is imposed on the cylinder with a low velocity, of the order of 10%, compared to the velocity of the flow. The problem data are the same as those used by Brooks and Hughes in (Brooks and Hughes 1982) and the results are shown for qualitative purposes only. The mesh of the fluid is less refined than in the previous examples: 1200 Taylor-Hood elements Q2Q1 and 4941 nodes were used (see Figure 13).

The time was discretized using the first order Euler Implicit method and at 0.05 second intervals. At least two iterations were computed by time increment. At 26 seconds of simulation, a symmetrical solution with two parallel and self-equilibrated vortices is observed in the cylinder mat, as shown in Figure 14 (a) and (b).

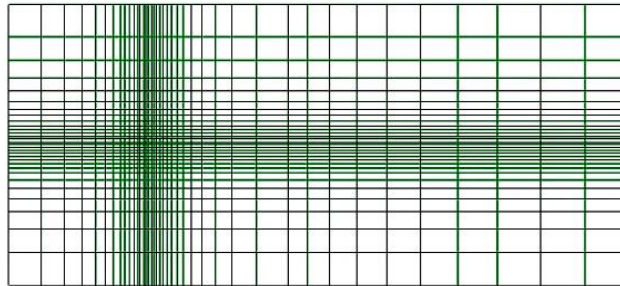
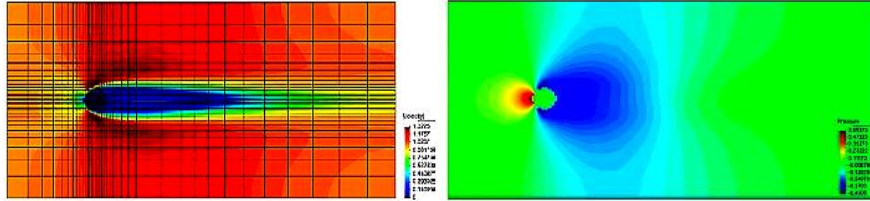
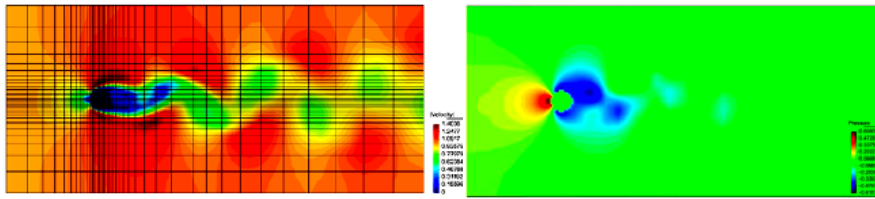


Figure 13. Mesh used in Problem 5.2: 1200 Taylor-Hood elements Q2Q1 and 4941 nodes



(a) speed field. Symmetric solution for $t=26s$. (b) Pressure field. Symmetric solution for $t=26s$.



(c) Speed range. Solution for $t = 94 s$. (d) Pressure field. Solution for $t = 94 s$.

Figure 14. Velocity and pressure contours obtained for the problem of transient flow around a cylinder with $Re=100$. (a) and (b) are symmetric solutions for $t=26sec$; (c) and (d) are solutions after stabilization of vortexing at $t=94 sec$

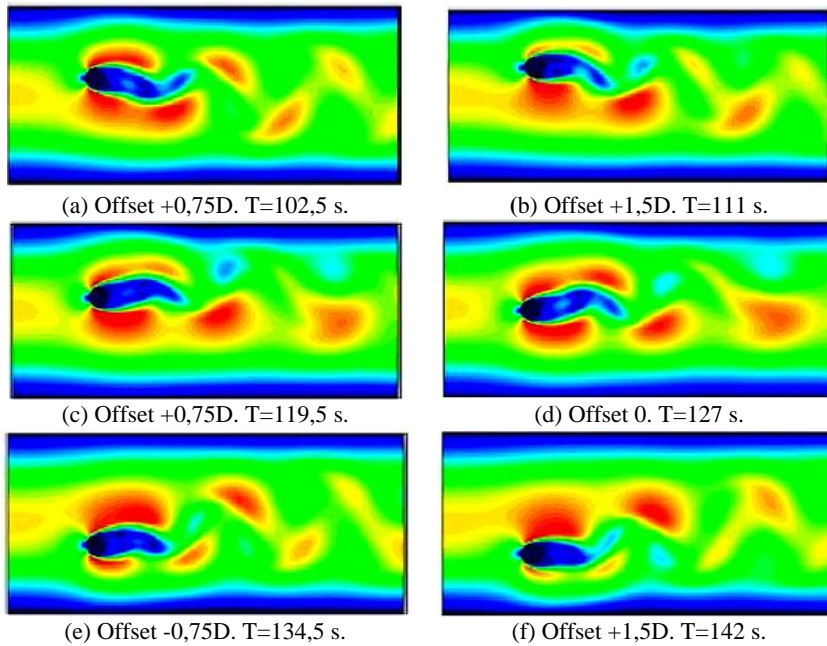


Figure 15. Velocity field for several instants of time of the moving cylinder

Figure 14 (c) and (d) shows the flow already stabilized after 94 seconds of simulation. From this moment, a vertical movement is imposed on the cylinder upwards until its center reaches a distance of $1.5D$ (where D is the cylinder diameter) from its initial position and, in the sequence, a downward movement is imposed until center reaches the position of $1.5D$ below the initial position. Finally, the cylinder is driven to its initial position. Figure 55 illustrates the velocity field at various instants of time for the reader to realize the overall movement of the cylinder. In the legends, the position of the cylinder is identified by the offset from the starting position. The results of Figure 15 are only for qualitative purposes because of the relatively coarse mesh and the large Δt that were used.

3.3. Stationary flow in a channel with elastic obstacle

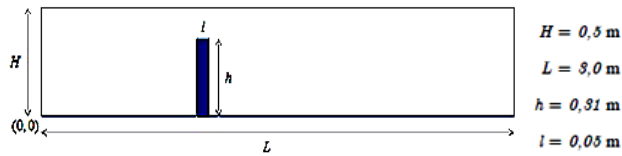


Figure 16. Schematic drawing of Problem 3.3

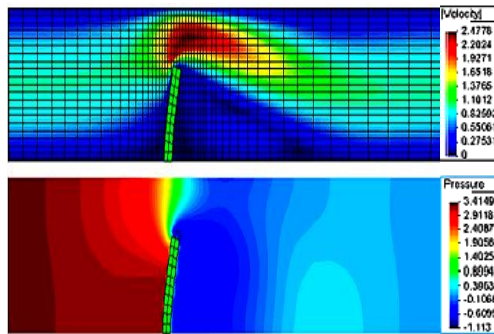


Figure 17. Speed and pressure fields of Problem 3.3.

This is a very simple example and consists of a steady flow in a channel with an elastic bar as an obstacle to the passage of the fluid, as shown in the Figure 16. The boundaries at the top and bottom of the channel have prescribed velocities equal to zero. At the output, free contour condition (zero stress) is assumed. The vertical velocity at the channel entrance is zero while the horizontal velocity has a parabolic profile with zero at the extremities and 1.0 m/s at the mean height. The density and kinematic viscosity are $\rho = 1.0 \text{ kg/m}^3$ and $\nu = 1.0 \text{ m}^2/\text{s}$, respectively, and the fluid domain was again discretized with Taylor-Hood elements Q2Q1. The structural domain was discretized with 20 quadrilateral elements of 9 nodes in a plane state of

deformation. The material is Neo-Hookian of Ciarlet-Simo with modulus of elasticity $E = 5200 \text{ N/m}^2$ and Poisson coefficient $\nu = 0,48$. Figure 17 shows the velocity and pressure results after convergence of the interface position in the coupled Fluid-Structure Interaction problem. Again these results are for qualitative purposes only.

4. Discussion and conclusions

It can be concluded that the challenge proposed as the objective of this paper was successfully achieved. The numerical examples solved proved that the formulation and implementation in finite elements developed in this work are capable of

- (1) Solve problems of 2D flow of fluids described by the Navier-Stokes equation for incompressible flows, even in regimes with dominant convection;
- (2) Simulation of fluid problems with mobile interfaces using the concept of boundaries immersed in two dimensions;

The use of discontinuous functions to interpolate the Lagrangian Multipliers along the interface, coupled with a discretization of the interface independent of the mesh of the fluid, provided results free of possible numerical instabilities, thus dispensing with additional stabilizations to the formulation and is perhaps the strength of this work. The construction of a mesh of Lagrange Multipliers independent of the fluid mesh, besides flexibilizing the size of the approximation subspace of this variable, minimizes the deleterious effect that is obtained when cutting a fluid element very close to one of its vertices. Another advantage of using discontinuous interpolation among the Lagrange Multipliers is the simplification of the computational code, since it facilitates the computation of the integrated terms along the interface.

As a possible improvement to be incorporated into this work in future projects we can highlight the improvement of the coupling method which has a slow convergence rate. In general, the number of iterations required for each time step has ranged from five to fifteen iterations in the problems analyzed. Another improvement that can be thought is with respect to the geometric algorithm of identification of the elements intersected by the interface and calculation of its contributions to the equations system. Occasionally, singularities in the mesh are identified, especially in long simulations such as those in Problem 3.2, and the solution adopted to overcome this difficulty was the modification of the time increment.

References

- Akkerman I., Dunaway J., Kvandal J., Spinks J., Bazilevs Y. (2012). Toward free-surface modeling of planing vessels: simulation of the Fridsma hull using ALE-VMS. *Computational Mechanics*, Vol. 50, No. 6, pp. 719-727. <https://doi.org/10.1007/s00466-012-0770-2>

- Bazilevs Y., Calo V. M., Hughes T. J., Zhang Y. (2008). Isogeometric fluid-structure interaction: theory, algorithms, and computations. *Computational Mechanics*, Vol. 43, No. 1, pp. 3-37. <https://doi.org/10.1007/s00466-008-0315-x>
- Bazilevs Y., Gohean J., Hughes T. J. R., Moser R. D., Zhang Y. (2009). Patient-specific isogeometric fluid–structure interaction analysis of thoracic aortic blood flow due to implantation of the Jarvik 2000 left ventricular assist device. *Computer Methods in Applied Mechanics and Engineering*, Vol. 198, No. 45-46, pp. 3534-3550. <https://doi.org/10.1016/j.cma.2009.04.015>
- Braess H, Wriggers P. (2000). Arbitrary Lagrangian Eulerian finite element analysis of free surface flow. *Comput. Computer Methods in Applied Mechanics and Engineering*, Vol. 190, pp. 95-109. [https://doi.org/10.1016/S0045-7825\(99\)00416-8](https://doi.org/10.1016/S0045-7825(99)00416-8)
- Brooks A. N., Hughes T. J. R. (1982). Streamline upwind/prestov-galerkin formulations fo convective dominated flows with particular emphasis on the incompressible navier-stokes equations. *Computer Methods in Applied Mechanics and Engineering*, Vol. 32, pp. 199-259. [https://doi.org/10.1016/0045-7825\(82\)90071-8](https://doi.org/10.1016/0045-7825(82)90071-8)
- Buscaglia G. C., Ausas R. F. (2011). Variational formulations for surface tension, capillarity and wetting. *Comput. Methods Appl. Mech. Engrg.* Vol. 200, pp. 3011-3025. <https://doi.org/10.1016/j.cma.2011.06.002>
- Dettmer W., Peric D. (2006). A computational framework for free surface fluid flows accounting for surface tension. *Comput. Methods Appl. Mech. Engrg.* Vol. 195, pp. 3038-3071. <https://doi.org/10.1016/j.cma.2004.07.057>
- Elias R. N., Coutinho A. L. G. A. (2009). Computational techniques for stabilized edge-based finite element simulation of nonlinear free-surface flows. *J. Offshore Mech. Arct. Eng.*, Vol. 54, No. 6-8, pp. 965-993. <https://doi.org/10.1002/flid.1475>
- Feng Y. T., Peric D. (2000). A time-adaptive space-time finite element method for incompressible Lagrangian flows with free surfaces: computational issues. *Comput. Methods Appl. Mech. Engrg.*, Vol. 190, No. 5, pp. 499-518. [https://doi.org/10.1016/S0045-7825\(99\)00425-9](https://doi.org/10.1016/S0045-7825(99)00425-9)
- Förster C., Wall W. A., Ramm E. (2007). Artificial added mass instabilities in sequential staggered coupling of nonlinear structures and incompressible viscous flows. *Comput. Methods Appl. Mech. Engrg.*, Vol. 196, No. 7, pp. 1278-1293. <https://doi.org/10.1016/j.cma.2006.09.002>
- Gerstenberger A., Wall W. A. (2010). An embedded Dirichlet formulation for 3D continua. *Int. J. Numer. Meth. Engng*, Vol. 82, No. 5, 537-563. <https://doi.org/10.1002/nme.2755>
- Gerstenberger A., Wall W. A. (2008). An eXtended Finite Element Method/Lagrange multiplier based Approach for Fluid-Structure Interaction. *Comput. Methods Appl. Mech. Engrg.*, Vol. 197, No. 19, pp. 1699-1714. <https://doi.org/10.1016/j.cma.2007.07.002>
- Idelsohn S. R., Marti J., Limache A., Oñate E. (2008). Unified Lagrangian Formulation for Elastic Solids and Incompressible Fluids: Application to Fluid–Structure Interaction Problems via the PFEM. *Comput. Methods Appl. Mech. Engrg.*, Vol. 197, No. 19-20, pp. 1762-1776. <https://doi.org/10.1016/j.cma.2007.06.004>
- Idelsohn S. R., Oñate E., Pin F. D., Calvo N. (2006). Fluid–Structure Interaction using the Particle Finite Element Method. *Comput. Methods Appl. Mech. Engrg.*, Vol. 195, pp. 2100-2123.

- Idelsohn S. R., Storti M. A., Oñate E. (2001). Lagrangian formulations to solve free surface incompressible inviscid fluid flows. *Comput. Methods Appl. Mech. Engrg.*, Vol. 191, pp. 583-593. [https://doi.org/10.1016/S0045-7825\(01\)00303-6](https://doi.org/10.1016/S0045-7825(01)00303-6)
- Kulasegaram S., Bonet J., Lewis R. W., Profit M. A. (2004). A variational formulation based contact algorithm for rigid boundaries in two-dimensional SPH applications. *Comput. Mech.*, Vol. 33, pp. 316-325. <https://doi.org/10.1007/s00466-003-0534-0>
- Küttler U., Wall W. A. (2008). Fixed-point fluid-structure interaction solvers with dynamic relaxation. *Comput. Mech.*, Vol. 43, pp. 61-72. <https://doi.org/10.1007/s00466-008-0255-5>
- Legay A., Chessa J., Belytschko T. (2006). An Eulerian-Lagrangian method for fluid-structure interaction based on level sets. *Comput. Methods Appl. Mech. Engrg.*, Vol. 195, pp. 2070-2087. <https://doi.org/10.1016/j.cma.2005.02.025>
- Lew A. J., Buscaglia G. C. (2008). A discontinuous-Galerkin-based immersed boundary method. *Int. J. Numer. Meth. Engrg.*, Vol. 76, pp. 427-454. <https://doi.org/10.1051/m2an/2010069>
- Lins E. F., Elias R. N., Rochinha F. A., Coutinho A. L. G. A. (2010). Residual-based variational multiscale simulation of free surface flows. *Comput. Mech.*, Vol. 46, pp. 545-557. <https://doi.org/10.1007/s00466-010-0495-z>
- Löhner R., Yang C., Oñate E. (2006). On the simulation of flows with violent free surface motion. *Comput. Methods Appl. Mech. Engrg.* Vol. 195, pp. 5597-5620. <https://doi.org/10.1016/j.cma.2005.11.010>
- Maier A., Gee M. W., Reeps C., Pongratz J., Eckstein H. H., Wall W. A. (2010). A comparison of diameter, wall stress, and rupture potential index for abdominal aortic aneurysm rupture risk prediction. *Annals of Biomedical Engineering*, Vol. 38, pp. 3124-3134. <https://doi.org/10.1007/s10439-010-0067-6>
- Marrone S., Antuono M., Colagrossi A., Colicchio G., Le-Touzé D., Graziani G. (2011). δ -SPH model for simulating violent impact flows. *Comput. Methods Appl. Mech. Engrg.* Vol. 200, pp. 1526-1542. <https://doi.org/10.1016/j.cma.2010.12.016>
- Moës N., Béchet E., Tourbier M. (2006). Imposing Dirichlet boundary conditions in the extended finite element method. *Int. J. Numer. Methods Engrg.* Vol. 67, pp. 1641-1669. <https://doi.org/10.1002/nme.1675>
- Oñate E., García J. (2001). A finite element method for fluid-structure interaction with surface waves using a finite calculus formulation. *Comput. Methods Appl. Mech. Engrg.* Vol. 191, pp. 635-660. [https://doi.org/10.1016/S0045-7825\(01\)00306-1](https://doi.org/10.1016/S0045-7825(01)00306-1)
- Oñate E., Idelsohn S. R., Celigueta M. A., Rossi R. (2008). Advances in the Particle Finite Element Method for the Analysis of Fluid-Multibody Interaction and Bed Erosion in Free Surface Flows. *Comput. Methods Appl. Mech. Engrg.* Vol. 197, pp. 1777-1800. <https://doi.org/10.1016/j.cma.2007.06.005>
- Rüberg T., Cirak F. (2012). Subdivision-stabilised immersed b-spline finite elements for moving boundary flows. *Comput. Methods Appl. Mech. Engrg.* Vol. 209-212, pp. 266-283. Retrieved from <https://doi.org/10.1016/j.cma.2011.10.007>
- Sanders J. D., Laursen T. A., Puso M. A. (2012). A Nitsche embedded mesh method. *Comput. Mech.* Vol. 49, pp. 243-257. <https://doi.org/10.1007/s00466-011-0641-2>

- Sawada T., Tezuka A. (2010). High-order Gaussian quadrature in X-FEM with the Lagrange Multiplier for fluid-structure coupling. *Int. J. Numer. Meth. Fluids* Vol. 64, pp. 1219-1239. <https://doi.org/10.1002/flid.2343>
- Schäfer M., Turek S. (1996). Benchmark computations of laminar flow around a cylinder. *Notes Numer. Fluid Mech.* Vol. 52, pp. 547-566. https://doi.org/10.1007/978-3-322-89849-4_39
- Takizawa K., Yabe T., Tsugawa Y., Tezduyar T., Mizoe H. (2007). Computation of free-surface flows and fluid-object interactions with the CIP method based on adaptive meshless soroban grids. *Comput. Mech.* Vol. 40, pp. 167-183. <https://doi.org/10.1007/s00466-006-0093-2>
- Takizawa K., Christopher J., Tezduyar T. E., Sathe S. (2010). Space-time finite element computation of arterial fluid-structure interactions with patient-specific data. *Int. J. Numer. Meth. Biomed. Engng.* Vol. 26, pp. 101-116. <https://doi.org/10.1002/cnm.1241>
- Tezduyar T. E., Osawa Y. (2000). Finite Element Stabilization Parameters Computed from Element Matrices and Vectors. *Comput. Methods Appl. Mech. Engrg.* Vol. 190, pp. 411-430. [https://doi.org/10.1016/S0045-7825\(00\)00211-5](https://doi.org/10.1016/S0045-7825(00)00211-5)
- Tezduyar T. E., Takizawa K., Brummer T., Chen P. R. (2011). Space-time fluid-structure interaction modeling of patient-specific cerebral aneurysms. *Int. J. Numer. Meth. Biomed. Engng.* Vol. 27, pp. 1665-1710. https://doi.org/10.1007/978-94-007-7769-9_2
- Torii R., Oshima M., Kobayashi T., Takagi K., Tezduyar T. (2011). Influencing factors in image-based fluid-structure interaction computation of cerebral aneurysms. *Int. J. Numer. Meth. Fluids*, Vol. 65, pp. 324-340. <https://doi.org/10.1002/flid.2448>
- Torii R., Oshima M., Kobayashi T., Takagi K., Tezduyar T. (2007). Numerical investigation of the effect of hypertensive blood pressure on cerebral aneurysm—Dependence of the effect on the aneurysm shape. *Int. J. Numer. Meth. Fluids*, Vol. 54, pp. 995-1009. <https://doi.org/10.1002/flid.1497>
- Torii R., Oshima M., Kobayashi T., Takagi K., Tezduyar T. (2009). Fluid-structure interaction modeling of blood flow and cerebral aneurysm: Significance of artery and aneurysm shapes. *Comput. Methods Appl. Mech. Engrg.* Vol. 198, pp. 3613-3621. <https://doi.org/10.1016/j.cma.2008.08.020>
- Turek S., Hron J., Razzaq M., Wobker H., Schäfer M (2010). Numerical Benchmarking of Fluid-Structure Interaction: A comparison of different discretization and solution approaches. *Lecture Notes in Computational Science and Engineering*, Vol. 73, pp. 413-424. https://doi.org/10.1007/978-3-642-14206-2_15
- Zienkiewicz O. C., Taylor R. L. (2009). The finite element method. fluid dynamics. Vol. 3.
- Zhaosheng Y. (2005). A DLM/FD method for fluid/flexible-body interactions. *J. Comput. Phys.*, Vol. 207, pp. 1-27.
- Zilian A., Fries T. P. (2009). A localized mixed-hybrid method for imposing interfacial constraints in the extended finite element method (XFEM). *Int. J. Numer. Meth. Engrg.* Vol. 79, pp. 733-752. <https://doi.org/10.1002/nme.2596>
- Zilian A., Legay A. (2008). The enriched space-time finite element method (EST) for simultaneous solution of fluid-structure interaction. *Int. J. Numer. Meth. Engrg.* Vol. 75, pp. 305-334. <https://doi.org/10.1002/nme.2258>